Identification of galectin-10 as a biomarker for periodontitis based on proteomic analysis of gingival crevicular fluid

JUN SU KIM[1*], IL-HOON CHO[2*], KYUNG-HEE KIM[3] and YOUNG SUN HWANG[4]

[1]Seoul Hana Dental Clinic; [2]Department of Biomedical Laboratory Science, College of Health Science, Eulji University, Seongnam, Gyeonggi 13135; [3]Proteomics Core Facility, Research Core Center, Research Institute, National Cancer Center, Goyang, Gyeonggi 10408; [4]Department of Dental Hygiene, College of Health Science, Eulji University, Seongnam, Gyeonggi 13135, Republic of Korea

Received July 28, 2020; Accepted October 28, 2020

DOI: 10.3892/mmr.2020.11762

Abstract. Periodontitis is a chronic inflammatory disease caused by the gradual breakdown of tissues surrounding the teeth due to various factors. The disease has been frequently noted in dental outpatients for a number of years. Improvements are required to current diagnostic methods, which have limitations in assessing the condition and progression of periodontitis. The development of diagnostic biomarkers for periodontitis to increase the sensitivity and accuracy of diagnosis is important for the management of periodontitis. In the present study, whole gingival crevicular fluid (GCF) from patients with periodontitis and healthy individuals was characterized via liquid chromatography with tandem mass spectrometry. Label-free quantification was used to identify the differentially abundant protein biomarkers. A total of 1,295 proteins were identified from the whole GCF of patients with periodontitis and healthy individuals via proteomic analysis. When analyzing biological processes, 'metabolic process' and 'cell organization and biogenes' were identified to play important roles in GCF under periodontitis conditions according to Gene Ontology. When analyzing molecular functions, 'catalytic activity' and 'protein binding' were the terms most enriched with differentially abundant proteins under periodontitis conditions. Galectin-10 (Gal-10) was one of the most upregulated proteins in the GCF of patients with periodontitis. The levels of prostaglandin E_2 were increased in oral keratinocytes and gingival fibroblasts treated with recombinant (r)Gal-10. The levels of interleukin-8, matrix metalloproteinase 9 and C-reactive protein were increased in the conditioned media (CM) of rGal-10-treated gingival fibroblasts. In addition, the CM of rGal-10-treated gingival fibroblasts induced osteoclast differentiation. These results suggested that Gal-10 expression was increased in the GCF of patients with periodontitis and contributed to the process of osteoclastogenesis. Therefore, Gal-10 may be a candidate biomarker for periodontitis.

Correspondence to: Professor Young Sun Hwang, Department of Dental Hygiene, College of Health Science, Eulji University, 553 Sansung-Daero, Sujeong-Gu, Seongnam, Gyeonggi 13135, Republic of Korea
E-mail: kiteys@eulji.ac.kr

*Contributed equally

Abbreviations: GCF, gingival crevicular fluid; Gal-10, galectin-10; PGE_2, prostaglandin E2; IL, interleukin; MMP, matrix metalloproteinase; CRP, C-reactive protein; CM, conditioned media; RANKL, receptor activator of NF-κB ligand; TRAP, tartrate-resistant acid phosphatase

Key words: GCF, periodontitis, proteome, biomarker, Gal-10, osteoclastogenesis

Introduction

Periodontal disease, also known as gum disease, is a major dental inflammatory disease with very high prevalence; in 2017, the number of patients with gingivitis and periodontal disease doubled in the Republic of Korea compared with the 7.94 million cases reported in 2010 (1). In 2019, 6.45 million patients were reported to have dental caries, higher than the 5.34 million reported in 2010 (2). Periodontal disease has been frequently noted as a dental outpatient disease for numerous years; Google Trends search results for global epidemiology and a global search of oral problems showed that the prevalence of dental caries and severe periodontitis is steadily increasing, making it the most common disease affecting humans worldwide (3,4). Periodontal disease is characterized by inflammatory lesions in tissues such as the gingival sulcus around the teeth that are caused by bacteria on the dental surface (5). In particular, endotoxins (such as lipopolysaccharides), exotoxins, flagella, antibiotic resistance and proteolytic activity can increase the risk of periopathogenic bacteria (6). Periodontal disease is caused by a combination of factors, including bacterial growth, nutrition, innate immunity, and endocrine and systemic disease factors. Periodontal disease can increase the periodontal pocket depth, and degrade periodontal ligaments and alveolar bone, leading to tooth loss (7).

In the early stages of periodontitis, patients may not be aware of the symptoms; however, as inflammation progresses, redness or bleeding gums while brushing and

gingival recession occur, resulting in the apparent lengthening of teeth (8). Deep pockets between the teeth develop as the gums are gradually destroyed due to inflammation of the connective tissue surrounding the teeth, eventually leading to tooth loss (8). Measurements of the probing depth of the periodontal pocket, the clinical attachment levels of the periodontal ligaments to the tooth surface, and dental radiography have been used as traditional diagnostic methods for periodontal disease (9). However, these traditional diagnostics methods can only identify the existence of disease or its presence in the past; they are suboptimal for assessing the progression of active disease. An optimal diagnostic method for periodontal disease needs to be quantitative and reproducible, with high sensitivity and specificity. It should also be non-invasive, fast, easily available in clinical settings, and economical to handle, store and transport for analysis. A diagnostic method that has received substantial attention is the use of biomarkers from oral tissues and saliva (10). Biomarkers are substances that can be objectively measured as indicators of a normal biological condition, pathological progression, or pharmacological response to treatment (11). They can be used in diagnosing and categorizing the stages of a disease, determining prognosis, predicting clinical responses, and for other purposes.

The periodontal pocket is filled with a liquid called gingival crevicular fluid (GCF), which originates from the surrounding capillaries (12). GCF reflects the condition of the gingiva, and contains proteins derived from serum or cells at inflamed sites. Compared to plasma (pH 6.8-7.3), GCF is weakly acidic or weakly alkaline (pH 6.5-8.5) (12). There are neutrophils, lymphocytes, macrophages, serum, inflammation-related molecules, antibodies and bacteria-derived components in GCF (13). Therefore, it has a defense mechanism that can efficiently control inflammation of the surrounding tissues compared with saliva (13). When inflammation levels are increased in the surrounding tissues, the permeability of the blood vessels increases, thereby increasing the secretion of GCF, which can restore the homeostasis of the periodontal pockets (14). Several diagnostic biomarkers for periodontitis have been reported through GCF proteomic analysis (15). However, only a limited number of GCF proteins identified by gel electrophoresis have been applied to proteomic analysis. Studies identifying the diagnostic biomarkers for periodontitis remain insufficient. Thus, in the present study, liquid chromatography-tandem mass spectrometry (LC-MS/MS) was used to identify periodontitis biomarkers by comparing whole GCF protein profiles between patients with periodontitis and healthy individuals, with the aim of improving periodontal care for patients.

Materials and methods

Reagents. All reagents used for cell culture were purchased from Gibco (Thermo Fisher Scientific, Inc.). Anti-galectin-10 (Gal-10) antibody (cat. no. MAB5447) was purchased from R&D Systems, Inc. Recombinant (r)Gal-10 protein and a human Gal-10 ELISA kit (cat. no. NBP2-75319; Novus Biologicals, LLC) were purchased from Novus Biologicals, LLC. All chemicals used for experiments were of analytical grade. Recombinant mouse receptor activator of NF-κB ligand (RANKL) was purchased from Koma Biotech, Inc. Recombinant mouse macrophage colony-stimulating factor (M-CSF) was purchased from R&D Systems, Inc. DAPI was obtained from Sigma-Aldrich (Merck KGaA).

GCF collection and sample preparation. The sample size was calculated using G*Power sampling software (version 3.1.9.7 for Windows; http://www.gpower.hhu.de/en.html) with an α error of 5% and power of 95%, with 20/group determined as the required sample size. Additional samples were collected in each group to compensate for processing errors. GCF was collected from healthy individuals (n=23) and patients with periodontitis (n=55) without systemic complications at Seoul Hana Dental Clinic between July and September 2019 (Seongnam, South Korea) by a dentist. The healthy individual group consisted of participants with clinically healthy periodontal tissues (low scores of bleeding on probing in <10% of the sites, and no sites with probing depth >3 mm or clinical attachment loss). The participants in the periodontitis group had teeth presenting probing depths of ≥3 mm and clinical attachment loss of ≥3 mm. Excluding periodontitis, subjects with oral inflammation and pregnant women were excluded from participation. Written informed consent was provided by each patient enrolled in the study. The normal group consisted of 10 males and 13 females (age range, 21-53 years; mean age, 34.7±7.18 years). The periodontitis group consisted of 37 males and 18 females (age range, 33-72 years; mean age, 50.9±10.47 years). The present study was approved by the Institutional Review Board of Eulji University (approval no. EU19-62). GCF was collected from the periodontal pockets around the teeth with inflamed gingival tissue using absorbent paper points (Meta Biomed Co., Ltd.). The sample sites were dried and isolated from saliva contamination using cotton rolls. The absorbent paper points were gently inserted into the sulcus and left in place for 30 sec. The paper points visibly contaminated with blood were discarded. The paper points wetted with GCF were incubated in 100 μl of phosphate-buffered saline (PBS) in an Eppendorf tube with agitation for 30 min at 4˚C. The samples were then centrifuged at 4,000 x g for 10 min at 4˚C. The supernatant was used for analysis.

GCF proteome analysis. GCF samples (25 μg) were precipitated using cold acetone. The extracted proteins were dissolved with 5% SDS solubilization buffer (5% SDS, 50 mM tetraethylammonium bromide, pH 7.55). These protein samples were then digested using S-Trap™ micro spin columns (ProtiFi) according to the manufacturer's instructions. Briefly, the proteins were reduced with dithiothreitol, alkylated with iodoacetamide and acidified using 12% aqueous phosphoric acid. The acidified SDS lysate was mixed with S-Trap binding buffer, loaded into S-Trap microtubes, and centrifuged at 4,000 x g for 30 sec at room temperature. Digestion buffer containing MS-grade trypsin/Lys-C protease mix was added and incubated for 1 h. The digested peptides were then eluted and dried using a concentrator. The digested samples were dissolved 0.1% trifluoroacetic acid aqueous solution, loaded onto reversed-phase fractionation spin columns (Thermo Fisher Scientific, Inc.) and centrifuged at 3,000 x g for 2 min at room temperature, followed by elution of the peptides in

solution (5, 7.5, 10, 12.5, 15, 17.5, 20 or 50% acetonitrile in 0.1% triethylamine). The eluted peptides were evaporated using vacuum centrifugation to obtain eight fractionated peptides. The fractionated peptide samples were resuspended in 0.1% aqueous formic acid solution and analyzed with a Q Exactive™ HF-X hybrid quadrupole-Orbitrap mass spectrometer (Thermo Fisher Scientific, Inc.) coupled with an Ultimate 3000 RSLCnano system (Thermo Fisher Scientific, Inc.). These fractionated peptides (1 μg) were loaded onto a trap column (Acclaim PepMap C18 column; 100 μm x 2 cm; Thermo Fisher Scientific, Inc.), separated with multistep linear gradient from 5 to 24% solvent B (0.1% formic acid in ACN) for 170 min, 24 to 36% solvent B for 10 min at a flow rate 300 nl/min on analytical columns (EASY-Spray column; 75 μm x50 cm; Thermo Fisher Scientific, Inc.) at 40˚C, and sprayed into a nano-electrospray ionization source with an electrospray voltage of 2.1 kV. The Q Exactive HF-X mass analyzer was operated using a top 10 data-dependent method. Full MS scans were acquired over a range m/z 350-1800 with a mass resolution of 60,000 (at m/z 200). The AGC target value was $3x10^6$. The ten most intense peaks with charge states of ≥2 was fragmented in higher-energy collisional dissociation collision cells with a normalized collision energy of 28. Tandem mass spectra were acquired with an Orbitrap mass analyzer using a mass resolution of 15,000 at m/z 200.

Data analysis. All LC-MS/MS raw data files were analyzed using Proteome Discoverer 2.4 software (Thermo Fisher Scientific, Inc.) for protein identification and label-free quantification. SEQUEST-HT, part of the Proteome Discoverer 2.4 software, was used for database searching against the UniProt human database. The database searching parameters included a precursor ion mass tolerance of 10 ppm, a fragment ion mass tolerance of 0.02 Da, a fixed modification for carbamidomethyl cysteine and variable modifications for methionine oxidation. Database searching against the corresponding reversed database was also performed to evaluate the false discovery rate (FDR) of peptide identification. An FDR of <1% at the peptide level was obtained, with filtering using high peptide confidence and at least two unique peptides. Precursor Ions Quantifier, part of the Proteome Discoverer 2.4 software, was used for label-free quantitation of GCF samples. Unique and razor peptides were used for GCF protein quantitation, normalized with total peptide amounts. Gene Ontology (GO; http://geneontology.org/) analysis was conducted to classify the whole GCF proteome and proteins differentially expressed between the two groups.

SDS-PAGE and zymography. Whole proteins from blood serum and GCFs were quantified using the Bradford method. In total, 2 μl protein sample and 198 μl Bradford reagent [0.1 mg/ml Coomassie Brilliant Blue G-250, 5% (v/v) methanol, 8.5% H_3PO_4] was added and incubated at room temperature for 5 min. Absorbance was measured at 595 nm. Proteins (10 mg) were separated via 13% SDS-PAGE and stained with Coomassie Brilliant Blue overnight at room temperature. For zymograms, samples were separated in 10% SDS-PAGE containing 0.1% gelatin (w/v). These gels were washed with 2.5% Triton X-100 for 30 min at room temperature and then incubated in a buffer containing 10 mM $CaCl_2$, 0.01% NaN_3 and 50 mM Tris-HCl (pH 7.5) for 16 h at 37˚C. Gels were then stained with Coomassie Brilliant Blue at room temperature overnight. Gelatinolytic activities of the matrix metalloproteinases (MMPs) were detected as clear bands against a dark blue background.

Western blotting. Proteins (10 mg) were incubated with Laemmli loading buffer (Bio-Rad Laboratories, Inc.) supplemented with 5% β-mercaptoethanol at 100˚C for 5 min. Proteins were then separated via 15% SDS-PAGE and transferred to PVDF membranes (EMD Millipore). The membranes were blocked with 5% skim milk in PBS for 2 h at room temperature and subsequently incubated with Gal-10 antibody (1:1,000) in 5% skim milk overnight at 4˚C. Then, the membranes were incubated with horseradish peroxidase-conjugated secondary antibodies (1:3,000; cat. no. 7076; Cell Signaling Technology, Inc.) for 2 h at room temperature. The targeted proteins were visualized using an Enhanced Chemiluminescence Detection kit (Amersham; Cytiva). Human blood serum (cat. no. H4522; Sigma-Aldrich; Merck KGaA) and BSA (cat. no. B8667; Sigma-Aldrich; Merck KGaA) were loaded as control.

Cell culture. Immortalized human oral keratinocytes (IHOKs) and immortalized gingival fibroblasts (IGFs) were obtained from the Oral Cancer Institute at the Yonsei University of Dentistry, South Korea in passages 55-60 (16) were cultured in DMEM:F-12 (3:1 ratio) supplemented with 10% FBS in a humidified atmosphere of 5% CO_2 at 37˚C. Additionally, a total of 30 male ICR mice (5 mice/group/experiment; age, 4 weeks; weight, 21-25 g) were obtained from the Central Lab Animal (Seoul, South Korea) and maintained at 20-22˚C with 40-60% relative humidity on a regular 12 h light/dark cycle in specific pathogen-free conditions and free access to food and water. All mice were sacrificed via cervical dislocation without prior anesthesia as previously described (17-19) and the tibia were separated under sterile conditions. Every effort was made to minimize suffering. Death was confirmed based on the absence of a corneal reflex, a failure to detect respiration and the absence of a heart beat for >5 min. No mice died for other reasons during the experiment. Mouse bone marrow-derived macrophages (BMMs) were isolated from tibiae via Histopaque® density gradient centrifugation at 400 x g for 30 min at room temperature. BMMs were cultured in α-MEM (Gibco; Thermo Fisher Scientific, Inc.) containing 10% FBS, 1% penicillin/streptomycin, and 30 ng/ml M-CSF in a humidified atmosphere of 5% CO_2 at 37˚C. The study was performed in accordance with experimental protocols approved by the Animal Ethics Committee of Eulji University (approval no. EUIACUC17-18).

ELISA. Gal-10 levels in GCF were quantified using human Gal-10 ELISA kit according to the manufacturer's protocols. Conditioned media (CM) from IHOKs and IGFs were used for prostaglandin E_2 (PGE_2) quantification using a human PGE_2 kit (cat. no. KGE004B; R&D Systems, Inc.) according to the manufacturer's protocols. Briefly, 1 or 5 μg/ml rGal-10 used to treat IHOKs or IGFs for 16 h in 5% CO_2 at 37˚C, and CM from cells was harvested. Distilled water was added for control. The absorbance was measured with a Synergy™ HTX Multi-Mode Microplate Reader (BioTek Instruments, Inc.).

Antibody array. A Human Periodontal Disease Antibody Array kit (cat. no. AAH-PDD-1-2; RayBiotech, Inc.) was used to identify the inflammatory cytokines produced by stimulation of the IGFs with rGal-10. Then, 5 μg/ml rGal-10 was used to treat IGFs for 16 h in 5% CO_2 at 37˚C, and CM of the IGFs was harvested. Distilled water was added for control. CM was then incubated for 24 h with the antibody array membranes according to the manufacturer's instructions. The images were changed to grayscale in 8-bit to reduce the background, and relative signal intensities were obtained by measuring the pixel area in the region of interest using ImageJ software (version 1.49; National Institutes of Health).

Osteoclast formation assay. Isolated BMMs ($2x10^4$ cells/well) were cultured in a 96-well plate with α-MEM containing M-CSF (30 ng/ml), RANKL (10 ng/ml) and/or CM for 5 days in a humidified atmosphere of 5% CO_2 at 37˚C. The cultures were supplemented every 2 days with fresh medium. To detect osteoclast formation, the cells were fixed with 4% paraformaldehyde for 30 min at room temperature and stained for tartrate-resistant acid phosphatase (TRAP) using an Acid Phosphatase Leukocyte kit (cat. no. 387A; Sigma-Aldrich; Merck KGaA) according to the manufacturer's instructions. The total number of TRAP-positive multinucleated (≥3 nuclei) cells/well was counted under a light microscope (magnification, x40).

Fluorescence microscopy was used to evaluate the cell morphology and count the nuclei in the osteoclasts. After washing with PBS and fixing with 4% paraformaldehyde for 30 min at room temperature, the cells were permeabilized with 0.5% Triton-X-100 in PBS for 2 h and blocked with 10% BSA for 1 h at room temperature. Cytoskeletal actin was stained with Alexa Fluor® 647-Phalloidin (1:100; cat. no. A22287; Thermo Fisher Scientific, Inc.) overnight at 4˚C. After washing with PBS, the cell nuclei were stained with DAPI (500 nM) at room temperature for 5 min. The cells were then washed thoroughly with PBS and photographed with a fluorescence microscope (EVOS FL Cell Imaging System; Thermo Fisher Scientific, Inc.).

Statistical analysis. Statistical analyses were conducted using InStat GraphPad Prism 5.01 software (GraphPad Software, Inc.). Non-parametric Mann-Whitney tests were used to compare two groups. Non-parametric Kruskal-Wallis tests with Dunn's post hoc analysis were employed for multiple comparisons. The results are presented as the mean ± SEM. $P<0.05$ was considered to indicate a statistically significant difference.

Results

Protein analysis of GCFs from normal and periodontitis group in SDS-PAGE and zymography. A total of 78 subjects were included in the present study, including 23 subjects in the normal group and 55 subjects in the periodontitis group. To analyze the GCF proteomes via LC-MS/MS, GCF samples were collected with absorbent paper points in the gingival sulcus and harvested with PBS solution. The protein concentrations were then estimated using the Bradford method. As shown in Fig. 1, the protein concentration of the GCF in the periodontitis group was 3.76-fold higher compared with in the normal group. The GCF samples were analyzed via SDS-PAGE and gelatin zymography (Fig. 2). The protein band patterns of the GCF samples were different compared with blood serum. Different proteolytic activities of all three samples were observed via gelatin zymography.

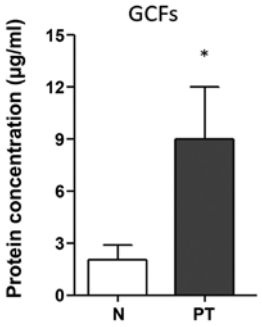

Figure 1. Protein concentration of GCF from healthy individuals and patients with periodontitis. Protein concentrations of GCFs were analyzed using the Bradford method. Normal (n=23), periodontitis (n=55). *P<0.05 vs. N. GCF, gingival crevicular fluid; N, normal healthy individuals; PT, periodontitis group.

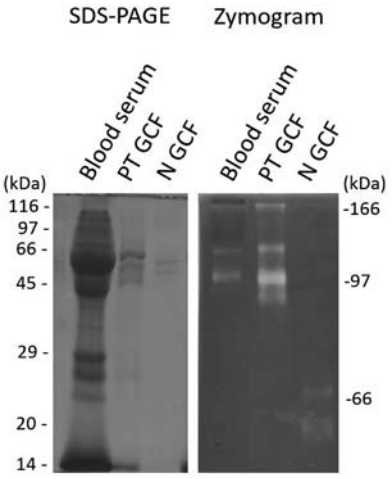

Figure 2. Validation of proteins and proteolytic activities of GCF from healthy individuals and patients with periodontitis. Proteins (10 μg) were analyzed using 13% SDS-PAGE. Proteolytic activities were analyzed using gelatin zymography (10% SDS-PAGE). Blood serum was loaded as a control. The experiments were repeated three times and representative results are shown for each experiment. GCF, gingival crevicular fluid; N, normal healthy individuals; PT, periodontitis group.

LC-MS/MS analysis of GCFs from normal and periodontitis group. GCF from the normal and periodontitis groups was separately pooled to prepare the amount of protein needed for LC-MS/MS analysis. The MS/MS raw data were searched against the human UniProt database using Proteome Discover. GO analysis was conducted to classify the whole GCF proteome and proteins differentially expressed between the two groups. By searching the UniProt human database using SEQUEST-HT with a protein identification criterion of at least two unique peptides per protein, 1,295 proteins were identified by the combined analysis of the GCF in the normal and periodontitis groups. Of these, 104 proteins were only

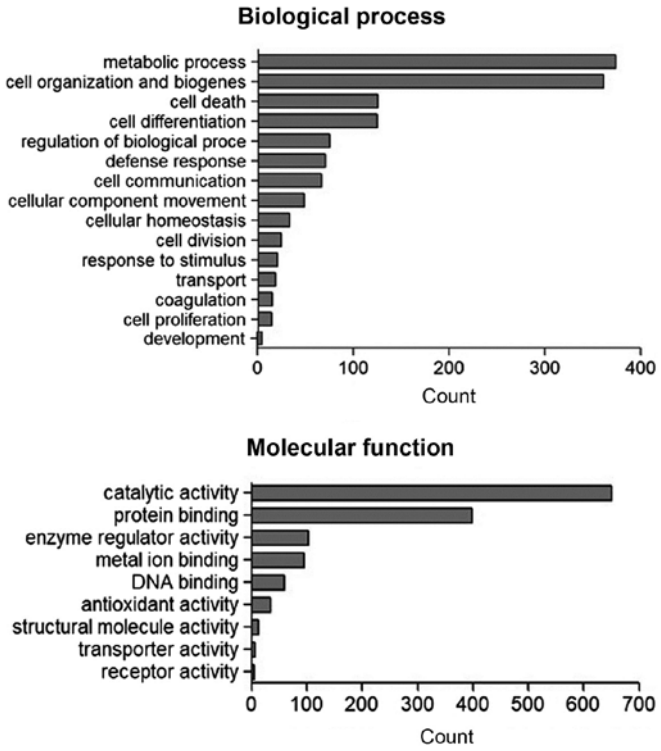

Figure 3. GCF proteomic analysis of differentially expressed proteins between the groups of healthy individuals and patients with periodontitis. Gene Ontology analysis was conducted to analysis the biological processes and molecular functions of the GCF proteome. GCF, gingival crevicular fluid.

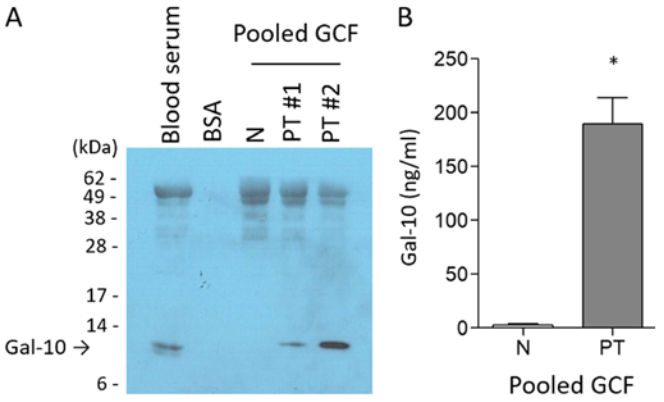

Figure 4. Validation of Gal-10 levels in pooled GCFs from healthy individuals and patients with periodontitis. (A) Gal-10 protein was analyzed via western blotting using pooled GCF, which was used for proteomic analysis. Blood serum and BSA were loaded as controls. (B) Protein levels of Gal-10 in the pooled GCFs were measured using a Gal-10 ELISA kit. *P<0.001 vs. N. Gal-10, galectin-10; GCF, gingival crevicular fluid; N, normal healthy individuals; PT, periodontitis group.

identified in GCF from the periodontitis group (Table I) and four proteins were only identified in the GCF from the normal group (Table II). GO analysis of biological processes identified 'metabolic process' and 'cell organization and biogenes' as the terms most enriched with proteins in GCF obtained under periodontitis conditions (Fig. 3). The molecular functions of the GCF proteome were also analyzed, with a special focus on catalytic activity and protein binding. After normalization of the spectral counts to the total ion currents, the average spectral counts of the analyses were calculated (duplicate analysis of two sets of experiments) for the normal and periodontitis samples, and then the fold change in the periodontitis group compared with the normal group was calculated. The results revealed that the average spectral counts of 228 proteins in the periodontitis group were increased by >5-fold (Table SI) and the average spectral counts of 138 proteins in the periodontitis group were decreased by >2-fold (Table SII).

Gal-10 increases the level of periodontal disease-associated cytokines. Among the proteins upregulated in periodontitis, a protein in the lectin family, Gal-10, was identified. Gal-10 has been suggested as a potential biomarker of eosinophilic airway inflammation (20). Gal-10 had a high ratio of average spectral counts in the periodontitis group. High levels of Gal-10 in the pooled periodontitis GCF were validated via western blotting using a Gal-10-specific antibody (Fig. 4A). Using ELISA, Gal-10 was found to be 76.5-fold higher in the pooled GCF of the periodontitis group (189 ng/ml) compared with in the healthy individual group (2.47 ng/ml; Fig. 4B). To observe the effect of Gal-10 on inflammation, the levels of PGE_2, a major end product of cyclooxygenase-2 in both acute and chronic inflammatory responses (21), were evaluated. rGal-10 was added to cultured IHOKs and IGFs, and the CM were analyzed for PGE_2 using ELISA. As shown in Fig. 5A, the PGE_2 levels were significantly increased in the CM from rGal-10-treated cells compared with in the controls. In the antibody array with human periodontal disease-associated cytokines, the levels of interleukin-8 (IL-8) and MMP-9 were significantly increased in the CM from rGal-10-treated IGF cultures (Fig. 5B). Compared with IL-8 and MMP-9, C-reactive protein (CRP) levels were increased to a lesser degree in CM from rGal-10-treated IGF cultures.

Gal-10 is involved in osteoclastogenesis. IL-8 (22), MMP-9 (23) and CRP (24) are intimately involved in osteoclastogenesis. Therefore, the effect of CM from rGal-10-treated cells on osteoclast differentiation was examined. CM from rGal-10-treated IGF cells was added to cultures of isolated BMMs. Osteoclast formation was then monitored. Based on fluorescence observation, CM stimulated monocyte fusion compared with the M-CSF alone. However, actin ring formation (represented by phalloidin staining) in CM-treated osteoclasts was defective compared with cells with added RANKL (10 ng/ml; Fig. 6). Using TRAP staining in the osteoclast formation assay, a greater number of TRAP-positive multinucleated cells were observed in the CM-treated cells compared with M-CSF treatment alone. CM induced TRAP-positive multinucleated cell formation, as much as observed in the RANKL treatment group. However, the number and relative size of the osteoclast actin rings were markedly lower than those with additional RANKL treatment. These results suggested that Gal-10 was involved in osteoclastogenesis via the induction of osteoclastogenic factors.

Discussion

In the present study, GCF from patients with periodontitis and healthy individuals was analyzed via LC-MS/MS to identify

Table I. Identified proteins in the gingival crevicular fluid of patients with periodontitis.

No.	Accession no.	Description [OS=*Homo sapiens*]	Sum PEP score	Coverage, %	Number of peptides	MW, kDa	Entrez gene ID	Gene symbol
1	Q9Y316-1	Protein MEMO1	61.029	29	6	33.7	51072	MEMO1
2	O95319-1	CUGBP Elav-like family member 2	60.057	13	5	54.3	10659	CELF2
3	Q14651	Plastin-1	56.509	11	7	70.2	5357	PLS1
4	P41439	Folate receptor γ	56.428	31	7	27.6	2352	FOLR3
5	A0A0C4DH32	Immunoglobulin heavy variable 3-20	40.176	43	4	12.7	28445	IGHV3-20
6	P84095	Rho-related GTP-binding protein RhoG	38.744	40	5	21.3	391	RHOG
7	Q9NP72	Ras-related protein Rab-18	38.382	42	7	23	22931	RAB18
8	O14745	Na(+)/H(+) exchange regulatory cofactor NHE-RF1	36.442	14	5	38.8	9368	SLC9A3R1
9	P08123	Collagen α-2(I) chain	33.435	4	4	129.2	1278	COL1A2
10	P61964	WD repeat-containing protein 5	32.844	19	5	36.6	11091	WDR5
11	Q9UM07	Protein-arginine deiminase type-4	31.771	13	6	74	23569	PADI4
12	Q8IZP2	Putative protein FAM10A4	29.619	23	4	27.4	145165	ST13P4
13	P05534	HLA class I histocompatibility antigen, A-24 α chain	27.857	16	4	40.7	3105	HLA-A
14	Q9Y263	Phospholipase A-2-activating protein	27.473	7	5	87.1	9373	PLAA
15	P19878	Neutrophil cytosol factor 2	26.768	9	4	59.7	4688	NCF2
16	P48960-1	CD97 antigen	25.288	9	4	91.8	976	CD97; ADGRE5
17	P78325-1	Disintegrin and metalloproteinase domain-containing protein 8	24.474	6	3	88.7	101	ADAM8
18	P62241	40S ribosomal protein S8	24.184	19	3	24.2	6202	RPS8
19	P08571	Monocyte differentiation antigen CD14	21.706	22	6	40.1	929	CD14
20	Q9H2H8-1	Peptidyl-prolyl cis-trans isomerase-like 3	21.607	29	4	18.1	53938	PPIL3
21	Q9Y3C6	Peptidyl-prolyl cis-trans isomerase-like 1	21.308	31	4	18.2	51645	PPIL1
22	P21266	Glutathione S-transferase Mu 3	20.419	15	3	26.5	2947	GSTM3
23	Q8WVV9	Heterogeneous nuclear ribonucleoprotein L-like	20.314	6	2	60	92906	HNRNPLL; HNRPLL
24	O15371	Eukaryotic translation initiation factor 3 subunit D	20.283	13	5	63.9	8664	EIF3D
25	P29144	Tripeptidyl-peptidase 2	20.133	5	5	138.3	7174	TPP2
26	P29692	Elongation factor 1-δ	19.528	13	3	31.1	1936	EEF1D
27	P07195	L-lactate dehydrogenase B chain	19.011	10	3	36.6	3945	LDHB
28	Q8IUI8	Cytokine receptor-like factor 3	18.661	9	4	49.7	51379	CRLF3
29	Q5JTV8	Torsin-1A-interacting protein 1	18.221	7	3	66.2	26092	TOR1AIP1
30	P06730	Eukaryotic translation initiation factor 4E	18.147	17	3	25.1	1977	EIF4E
31	Q13630	GDP-L-fucose synthase	18.14	12	3	35.9	7264	TSTA3
32	O95831-1	Apoptosis-inducing factor 1, mitochondrial	17.99	8	4	66.9	9131	AIFM1
33	P52789	Hexokinase-2	17.98	5	4	102.3	3099	HK2
34	Q15008	26S proteasome non-ATPase regulatory subunit 6	17.548	15	5	45.5	9861	PSMD6
35	P49458	Signal recognition particle 9 kDa protein	16.61	36	3	10.1	6726; 653226	SRP9; RP9P1
36	O60234	Glia maturation factor γ	16.521	27	3	16.8	9535	GMFG

Table I. Continued.

No.	Accession no.	Description [OS=*Homo sapiens*]	Sum PEP score	Coverage, %	Number of peptides	MW, kDa	Entrez gene ID	Gene symbol
37	P07814	Bifunctional glutamate/proline-tRNA ligase	16.224	2	2	170.5	2058	EPRS
38	Q14002-1	Carcinoembryonic antigen-related cell adhesion molecule 7	15.958	11	2	29.4	1087	CEACAM7
39	P02649	Apolipoprotein E	15.318	8	2	36.1	348	APOE
40	Q9BWS9-1	Chitinase domain-containing protein 1	15.165	7	2	44.9	66005	CHID1
41	P42768	Wiskott-Aldrich syndrome protein	14.674	6	2	52.9	7454	WAS
42	Q99832	T-complex protein 1 subunit eta	14.661	7	3	59.3	10574	CCT7
43	Q14444-1	Caprin-1	13.695	4	3	78.3	4076	CAPRIN1
44	P09874	Poly[ADP-ribose] polymerase 1	13.613	3	3	113	142	PARP1
45	Q9HA64	Ketosamine-3-kinase	13.281	13	4	34.4	79672	FN3KRP
46	P30419	glycylpeptide N-tetradecanoyltransferase 1	13.098	6	2	56.8	4836	NMT1
47	Q9BUT1-1	3-hydroxybutyrate dehydrogenase type 2	12.898	11	2	26.7	56898	BDH2
48	Q92608-1	Dedicator of cytokinesis protein 2	12.582	2	3	211.8	1794	DOCK2
49	P57737	Coronin-7	12.383	4	2	100.5	79585	CORO7
50	Q12765	Secernin-1	12.128	8	3	46.4	9805	SCRN1
51	Q9BRR6-1	ADP-dependent glucokinase	12.074	6	2	54.1	83440	ADPGK
52	P09429	High mobility group protein B1	12.035	28	3	24.9	3146	HMGB1
53	Q9BVM4	γ-glutamylaminecyclotransferase	11.945	17	2	17.3	87769	GGACT
54	P36639	7,8-dihydro-8-oxoguanine triphosphatase	11.726	13	2	22.5	4521	NUDT1
55	Q96EP5	DAZ-associated protein 1	11.593	8	2	43.4	26528	DAZAP1
56	A6NHR9-1	structural maintenance of chromosomes flexible hinge domain-containing protein 1	11.468	2	3	226.2	23347	SMCHD1
57	Q96GX9-1	Methylthioribulose-1-phosphate dehydratase	11.327	12	2	27.1	51074	APIP
58	P16144-1	Integrin β-4	10.934	2	3	202	3691	ITGB4
59	Q9Y4Z0	U6 snRNA-associated Sm-like protein LSm4	10.689	16	2	15.3	25804	LSM4
60	P06454-1	Prothymosin α	10.539	10	2	12.2	5757	PTMA
61	P51572	B-cell receptor-associated protein 31	10.493	8	2	28	10134	BCAP31
62	Q9BUL8	programmed cell death protein 10	10.433	16	3	24.7	11235	PDCD10
63	O00203-1	AP-3 complex subunit β-1	10.211	3	2	121.2	8546	AP3B1
64	Q9BTT0	Acidic leucine-rich nuclear phosphoprotein 32 family member E	10.148	10	2	30.7	81611	ANP32E
65	P45973	chromobox protein homolog 5	10.089	11	2	22.2	23468	CBX5
66	P51688	N-sulphoglucosamine sulphohydrolase	10.015	5	2	56.7	6448	SGSH
67	O43639	Cytoplasmic protein NCK2	9.844	9	3	42.9	8440	NCK2
68	Q96D96-1	voltage-gated hydrogen channel 1	9.622	10	2	31.7	84329	HVCN1
69	Q07812	Apoptosis regulator BAX	9.537	14	2	21.2	581	BAX
70	Q14314	Fibroleukin	9.444	7	2	50.2	10875	FGL2
71	P48507	Glutamate-cysteine ligase regulatory subunit	9.386	9	2	30.7	2730	GCLM
72	P39023	60S ribosomal protein L3	9	6	2	46.1	6122	RPL3
73	P62906	60S ribosomal protein L10A	8.762	10	2	24.8	4736	RPL10A
74	Q8N3Y7-1	epidermal retinol dehydrogenase 2	8.748	9	3	34.1	195814	SDR16C5

Table I. Continued.

No.	Accession no.	Description [OS=*Homo sapiens*]	Sum PEP score	Coverage, %	Number of peptides	MW, kDa	Entrez gene ID	Gene symbol
75	Q13627-1	Dual specificity tyrosine-phosphorylation-regulated kinase 1A	8.632	3	2	85.5	1859	DYRK1A
76	O15231-1	zinc finger protein 185	8.471	3	2	73.5	7739	ZNF185
77	Q08170	Serine/arginine-rich splicing factor 4	8.421	4	2	56.6	6429	SRSF4
78	Q9UKG1	DCC-interacting protein 13-α	8.319	4	2	79.6	26060	APPL1
79	Q04206	Transcription factor p65	8.31	7	3	60.2	5970	RELA
80	P16284	Platelet endothelial cell adhesion molecule	8.275	3	2	82.5	5175	PECAM1
81	P31040	Succinate dehydrogenase [ubiquinone] flavoprotein subunit, mitochondrial	8.107	3	2	72.6	6389	SDHA
82	P57088	Transmembrane protein 33	8.101	9	2	28	55161	TMEM33
83	Q16543	Hsp90 co-chaperone Cdc37	8.046	5	2	44.4	11140	CDC37
84	Q9BR76	Coronin-1B	7.765	4	2	54.2	57175	CORO1B
85	Q7KZI7-1	Serine/threonine-protein kinase MARK2	7.539	2	2	87.9	2011	MARK2
86	Q14331	Protein FRG1	7.272	11	2	29.2	2483	FRG1
87	Q7L1Q6-1	Basic leucine zipper and W2 domain-containing protein 1	7.083	5	2	48	9689	BZW1
88	P18124	60S ribosomal protein L7	6.92	9	2	29.2	6129	RPL7
89	Q14155-1	Isoform 1 of Rho guanine nucleotide exchange factor 7	6.796	3	2	73.1	8874	ARHGEF7
90	O75663	TIP41-like protein	6.768	8	2	31.4	261726	TIPRL
91	Q9UIQ6-1	Leucyl-cystinyl aminopeptidase	6.63	2	2	117.3	4012	LNPEP
92	A4D1P6-1	WD repeat-containing protein 91	6.44	3	2	83.3	29062	WDR91
93	P63151	Serine/threonine-protein phosphatase 2A 55 kDa regulatory subunit B α isoform	6.305	5	2	51.7	5520	PPP2R2A
94	P35542	Serum amyloid A-4 protein	6.291	15	2	14.7	6291	SAA4
95	P62701	40S ribosomal protein S4, X isoform	6.247	7	2	29.6	6191	RPS4X
96	P62263	40S ribosomal protein S14	6.065	16	2	16.3	6208	RPS14
97	P16885	1-phosphatidylinositol 4,5-bisphosphate phosphodiesterase γ-2	5.98	2	2	147.8	5336	PLCG2
98	O00204	Sulfotransferase family cytosolic 2B member 1	5.707	6	2	41.3	6820	SULT2B1
99	Q99490	Arf-GAP with GTPase, ANK repeat and PH domain-containing protein 2	5.305	2	2	124.6	116986	AGAP2
100	P16949-1	Stathmin	4.854	14	2	17.3	3925	STMN1
101	O00232-1	26s proteasome non-atpase regulatory subunit 12	4.432	4	2	52.9	5718	PSMD12
102	Q15005	Signal peptidase complex subunit 2	4.361	8	2	25	9789	SPCS2
103	P16333-1	Cytoplasmic protein NCK1	4.185	5	2	42.8	4690	NCK1
104	P61254	60S ribosomal protein L26	3.973	10	2	17.2	6154	RPL26

MW, molecular weight; PEP, posterior error probability; OS, organism.

the proteins involved in periodontitis. Compared with normal serum, healthy GCF exhibited a notably reduced protein content. However, as inflammation processes, vascular permeability is increased, thereby increasing the inflow of various proteins, cell-mediated immune systems and humoral immune systems into the periodontal pocket (25). Therefore, GCF may be a useful target to elucidate the inflammatory state of periodontal disease. However, GCF quantities are typically very small and difficult to analyze. Nevertheless, quantitative protein measurements showed that the protein concentration

Table II. Identified proteins in the gingival crevicular fluid of healthy individuals.

No.	Accession no.	Description [OS=*Homo sapiens*]	Sum PEP score	Coverage, %	Number of peptides	MW, kDa	Entrez gene ID	Gene symbol
1	P19961	A-amylase 2B	553.082	74	31	57.7	280	AMY2B
2	Q15363	Transmembrane emp24 domain-containing protein 2	12.942	18	3	22.7	10959	TMED2
3	Q9UGM5-1	Fetuin-B	5.909	5	2	42	26998	FETUB
4	Q15782-4	Chitinase-3-like protein 2	5.868	6	2	43.5	1117	CHI3L2

MW, molecular weight; PEP, posterior error probability; OS, organism.

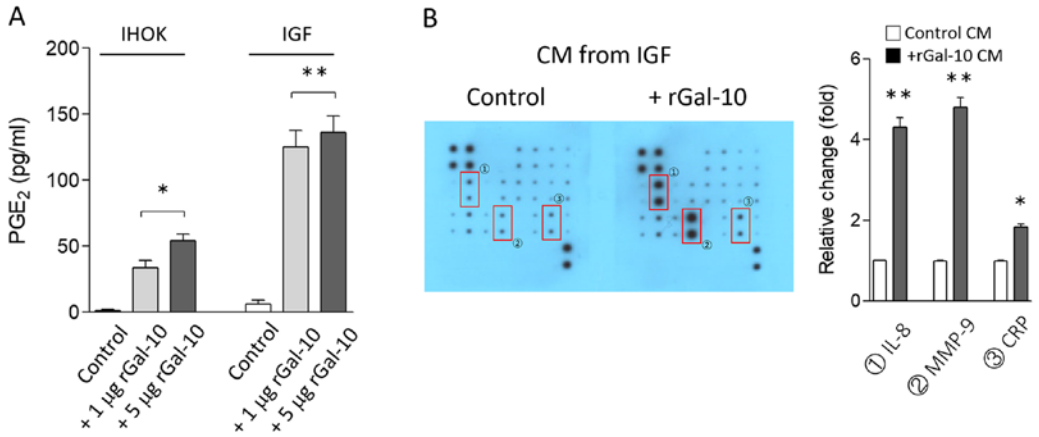

Figure 5. Analysis of inflammatory molecules after rGal-10 stimulation. (A) IHOK and IGF cells were treated with 5 μg/ml rGal-10 for 16 h and PGE_2 levels in the CM were analyzed using a PGE_2 ELISA kit. *P<0.05, **P<0.001 vs. control. (B) Periodontal antibody array was performed with the CM from rGal-10-stimulated IGFs. The relative array signal intensities were determined using ImageJ software. The cytokines with significant changes are indicated by circled numbers. *P<0.05, **P<0.001 vs. control CM. CM, conditioned media; CRP, C-reactive protein; IGF, immortalized gingival fibroblasts; IHOK, immortalized human oral keratinocytes; IL, interleukin; MMP, matrix metalloproteinase; PGE_2, prostaglandin E_2; rGal-10, recombinant galectin-10.

in the GCF of patients were periodontitis was significantly increased compared with in the GCF from healthy individuals in the present study. GCF components vary depending upon the periodontal microenvironment; thus, GCF may be useful for finding diagnostic markers for periodontitis. A number of studies have attempted to search for diagnostic biomarkers for periodontal disease using GCF (26,27); superoxide dismutase, apolipoprotein A-I, dermcidin, L-plastin, Annexin-1 and azurocidin have been suggested as diagnostic biomarkers from LC-MS/MS analysis of the GCF from patients with periodontitis and healthy individuals (28-30).

However, to the best of our knowledge, no study has performed a proteomic analysis to identify diagnostic biomarkers of periodontal disease using entire GCF samples; in previous studies, proteins in the GCF samples were separated via SDS-PAGE or 2-dimensional electrophoresis and stained, and only proteins with significant differences in expression between the control and patient samples were selected and subjected to proteomic analysis. Although this method can reduce noise in the LC-MS/MS analysis and increase the success rate of identifying diagnostic markers, low molecular weight proteins, which were not included in the separation gel, would have been excluded from the proteomic analysis. Although the sample size of GCF applied to the present analysis differed from previous studies, 238 (26), 230 (27), 327 (28), 154 (29) and 305 proteins (30) have been identified through protein screening process using electrophoresis. In the present study, GCF was directly collected from the gingival sulcus using absorption paper strips and all GCF collected was subjected to LC-MS/MS analysis. A total of 1,295 proteins were identified from the combined analysis of both the GCF of patients with periodontitis and healthy individuals; small proteins with molecular weights of 7.5-20 kDa were thus included. According to the GO analysis, for biological processes, 'metabolic process' and 'cell organization and biogenes' were the most significantly enriched processes in GCF under periodontitis conditions. Proteins involved in 'catalytic activity' and 'protein binding' were also enriched in GCF from patients with periodontitis according to GO analysis of molecular functions.

As only limited volumes of GCF containing low quantities of protein can be collected, the GCF samples were pooled to obtain enough protein for LC-MS/MS analysis. The main purpose of the GCF pooling strategy was to reduce the impact of individual variability in protein expression level as much as possible. However, the disadvantage of such a sample-pooling strategy was that tests for statistical significance could not be performed. Therefore, multiple LC-MS/MS analyses are required for pooled GCF samples. Of the 228 proteins showing >5-fold increases in the average

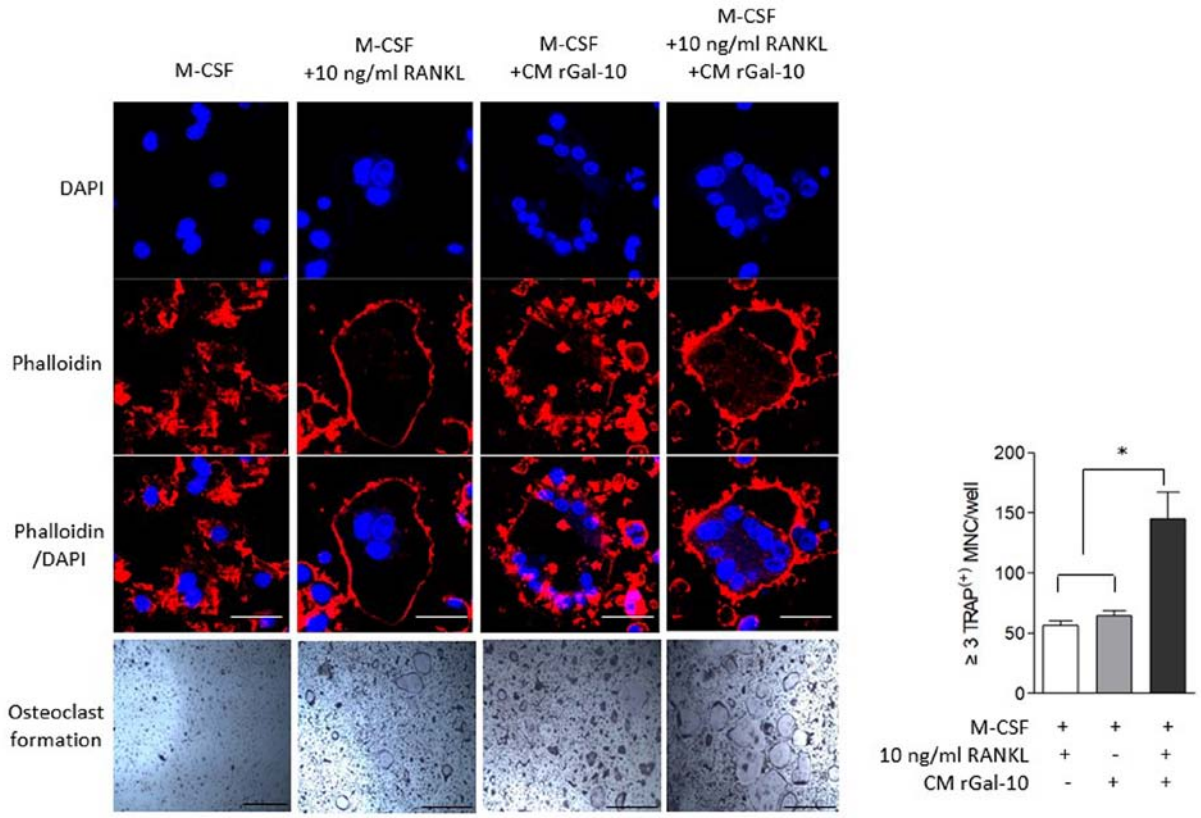

Figure 6. Effect of rGal-10 on osteoclastogenesis. To observe the morphology and nuclear numbers in osteoclasts, bone marrow-derived macrophages were treated with M-CSF (30 ng/ml), RANKL (10 ng/ml) and/or CM from rGal-10-stimulated IGFs for 5 days and stained for F-actin [with Alexa Fluor 647-phalloidin (red)], with DAPI staining (blue) used to visualize the nucleus. The cells were visualized and photographed with a fluorescence microscope. Magnification, x200. Scale bar, 50 μm. The osteoclast formation assay was also performed under the same conditions followed by TRAP staining. Staining was monitored via light microscopy. Magnification, x200. Scale bar, 50 μm. Representative results are shown for each experiment. The graph shows the total number of TRAP-positive multinucleated (≥3 nuclei) osteoclasts/well. The data are expressed as the mean ± SEM of three independent experiments. *P<0.001. CM, conditioned media; IGF, immortalized gingival fibroblast; M-CSF, macrophage colony-stimulating factor; MNC, multinuclear cell; RANKL, receptor activator of NF-κB ligand; rGal-10, recombinant galectin-10; TRAP, tartrate-resistant acid phosphatase.

spectral counts of the periodontitis group GCF, Gal-10 was identified and selected to validate its role in periodontitis. Galectins are carbohydrate-binding proteins that can recognize β-galactosides (31). A total of 15 isotypes of galectin have been reported in mammals (32). Galectins mostly accumulate in the cytoplasm, but are released after cell injury (33). Some galectin isotypes can also be secreted by activated immune cells and epithelial cells (32,33). Galectins have extensive functions, including mediating cell-cell interactions, cell-matrix adhesion and transmembrane signaling (32,33). In addition, galectins have functions in apoptosis, the suppression of T-cell receptor activation and nuclear pre-mRNA splicing (34,35). Gal-10 is expressed in eosinophils and basophils, and plays an essential role in the immune system by suppressing T cell proliferation (36). Several reports have suggested that galectin is involved in osteoclastogenesis, although this function was dependent upon the isotype of galectin (37-39).

In the present study, treatment with rGal-10 resulted in increased levels of the inflammatory response molecule PGE_2 in IHOK and IGF cells. In the CM from rGal-10-treated IGF culture, significant increases in IL-8, MMP-9 and CRP were detected using an antibody array. IL-8 (22), MMP-9 (23) and CRP (24) are intimately involved in inflammation and osteoclastogenesis. To observe the effect of Gal-10 on osteoclastogenesis, osteoclast differentiation was examined using an *in vitro* culture system. The CM from rGal-10-treated cell cultures significantly induced osteoclast formation, but defects in the actin-based cytoskeletal organization of the osteoclasts were observed compared with osteoclast formation in RANKL-treated culture. These results indicated that Gal-10 expression in GCF could be increased by periodontitis conditions and stimulate the release of cytokines related to osteoclast differentiation, thereby inducing osteoclast formation.

Biomarkers of periodontal disease may include the microbiological elements of periodontal pathogens, intermediate molecules of the host immune-inflammatory response, proteolytic molecules of connective tissues and bone remodeling molecules (40). As red complex bacteria in the subgingival space are highly associated with the occurrence and progression of periodontitis, the presence of periodontal pathogens themselves can be used as a biomarker for periodontitis (5,6,10). However, microbial periodontal pathogens may not cause periodontitis due to efficient host defense mechanisms; therefore, it is necessary to analyze other biomarkers rather than using microbial pathogenic biomarkers alone. Immunoglobulin, IL-1β, IL-6, tumor necrosis factor-α and β-glucuronidase have been proposed as biomarkers for host immune-inflammatory responses (41). IL-1β stimulates the secretion of various molecules involved in the destruction of tissues in inflammatory disease, suggesting towards its

positive association with periodontitis (13). MMPs, aspartate aminotransferase and tissue inhibitor of MMP have been also proposed as biomarkers used to diagnose moderate and aggressive periodontitis (13). RANKL, osteocalcin, osteonectin and osteopontin are bone remodeling-related biomarkers (13). GCF reflects changes in the periodontal microenvironment; therefore, GCF is an important target to use for the development of various diagnostic biomarkers with high sensitivity and accuracy.

The present study aimed to elucidate useful target markers for the diagnosis of periodontitis by analyzing the GCF proteins of patients with periodontitis. Gal-10 was suggested as a useful diagnostic biomarker for periodontitis by proteomic analyses of whole GCF from patients with periodontitis and healthy individuals. However, due to the limited number of participants, the protein levels of Gal-10 at different stages of periodontitis have not been verified. Further GCF proteomic analyses are required to evaluate the sensitivities of Gal-10 in differential stages of periodontitis in a larger cohort.

Proteins whose expression levels were altered during periodontitis were identified via LC-MS/MS analysis of whole GCF from patients with periodontitis and healthy individuals in the present study, and it was determined that Gal-10 protein levels were high in GCF from patients with periodontitis. Gal-10 contributed to osteoclastogenesis by inducing molecules related to inflammation and osteoclast differentiation. Therefore, Gal-10 can be considered a potential biomarker for periodontitis. Larger cohort studies are required to characterize the complete GCF proteome in health and disease.

Acknowledgements

Not applicable.

Funding

This research was supported by Eulji University in 2019 and the Basic Science Research Program through the National Research Foundation of Korea funded by the Ministry of Education, Science and Technology (grant no. 2018R1D1A1 B07042035).

Availability of data and materials

The datasets used and/or analyzed during the current study are available from the corresponding author on reasonable request.

Authors' contributions

YSH and IHC designed the study. JSK was involved in the sample collection, and YSH, JSK and IHC performed the experiments. YSH, JSK and KHK analyzed the data and YSH, JSK and IHC drafted the manuscript. All authors read and approved the final manuscript.

Ethics approval and consent to participate

Human experiments were approved by the Institutional Review Board of Eulji University (approval no. EU19-62). Written informed consent was provided by each patient in this study. Animal experiments were performed in accordance with experimental protocols approved by the Animal Ethics Committee of Eulji University (approval no. EUIACUC17-18).

Patient consent for publication

Not applicable.

Competing interests

The authors declare that they have no competing interests.

References

1. Ministry of Health and Welfare: Health Insurance Review and Assessment Service in Korea. 2017 Statistical Yearbook of Health Insurance. http://www.mohw.go.kr/react/al/sal0301vw.jsp?PAR_MENU_ID=04&MENU_ID=0403&CONT_SEQ=346196. Accessed July 24, 2019.
2. Health Insurance Review and Assessment Service in Korea: Healthcare Bigdata Hub. http://opendata.hira.or.kr/op/opc/olapHifrqSickInfo.do. Accessed November 12, 2020.
3. Frencken JE, Sharma P, Stenhouse L, Green D, Laverty D and Dietrich T: Global epidemiology of dental caries and severe periodontitis-a comprehensive review. J Clin Periodontol 44 (Suppl 18): S94-S105, 2017.
4. Patthi B, Kumar JK, Singla A, Gupta R, Prasad M, Ali I, Dhama K and Niraj LK: Global search trends of oral problems using google trends from 2004 to 2016: An exploratory analysis. J Clin Diagn Res 11: ZC12-ZC16, 2017.
5. Lertpimonchai A, Rattanasiri S, Arj-Ong Vallibhakara S, Attia J and Thakkinstian A: The association between oral hygiene and periodontitis: A systematic review and meta-analysis. Int Dental J 67: 332-343, 2017.
6. Teles R, Teles F, Frias-Lopez J, Paster B and Haffajee A: Lessons learned and unlearned in periodontal microbiology. Periodontol 62: 95-162, 2013.
7. Cekici A, Kantarci A, Hasturk H and Van Dyke TE: Inflammatory and immune pathways in the pathogenesis of periodontal disease. Periodontol 2000 64: 57-80, 2014.
8. Institute for Quality and Efficiency in Health Care (IQWiG): Gingivitis and periodontitis: Overview [Internet]. Last Update: February 27, 2020. IQWiG, Cologne, Germany. https://www.ncbi.nlm.nih.gov/books/NBK279593/.
9. Highfield J: Diagnosis and classification of periodontal disease. Aust Dent J 54 (Suppl 1): S11-S26, 2009.
10. Gupta S, Chhina S and Arora SA: A systematic review of biomarkers of gingival crevicular fluid: Their predictive role in diagnosis of periodontal disease status. J Oral Biol Craniofac Res 8: 98-104, 2018.
11. Mayeux R: Biomarkers: Potential uses and limitations. NeuroRx 1: 182-188, 2004.
12. Baliga S, Muglikar S and Kale R: Salivary pH: A diagnostic biomarker. J Indian Soc Periodontol 17: 461-465, 2013.
13. Barros SP, Williams R, Offenbacher S and Morelli T: Gingival crevicular fluid as a source of biomarkers for periodontitis. Periodontol 2000 70: 53-64, 2016.
14. Kurgan S and Kantarci A: Molecular basis for immunohistochemical and inflammatory changes during progression of gingivitis to periodontitis. Periodontol 2000 76: 51-67, 2018.
15. Subbarao KC, Nattuthurai GS, Sundararajan SK, Sujith I, Joseph J and Syedshah YP: Gingival crevicular fluid: An overview. J Pharm Bioallied Sci 11 (Suppl 2): S135-S139, 2019.
16. Illeperuma RP, Kim DK, Park YJ, Son HK, Kim JY, Kim J, Lee DY, Kim KY, Jung DW, Tilakaratne WM and Kim J: Areca nut exposure increases secretion of tumor-promoting cytokines in gingival fibroblasts that trigger DNA damage in oral keratinocytes. Int J Cancer 137: 2545-2557, 2015.
17. Hwang YH, Kim SJ, Kim SH and Yee ST: Physcion effectively mitigates ovariectomy-induced osteoporosis in mice. Med Drug Discovery 6: 100032, 2020.
18. Luo G, Li F, Li X, Wang ZG and Zhang B: TNF-α and RANKL promote osteoclastogenesis by upregulating RANK via the NF-κB pathway. Mol Med Rep 17: 6605-6611, 2018.

19. Lee D, Heo DN, Kim HJ, Ko WK, Lee SJ, Heo M, Bang JB, Lee JB, Hwang DS, Do SH and Kwon IK: Inhibition of osteoclast differentiation and bone resorption by bisphosphonate-conjugated gold nanoparticles. Sci Rep 6: 27336, 2016.
20. Chua JC, Douglass JA, Gillman A, O'Hehir RE and Meeusen EN: Galectin-10, a potential biomarker of eosinophilic airway inflammation. PLoS One 7: e42549, 2012.
21. Ricciotti E and FitzGerald GA: Prostaglandins and inflammation. Arterioscler Thromb Vasc Biol 31: 986-1000, 2011.
22. Herrero AB, García-Gómez A, Garayoa M, Corchete LA, Hernández JM, San Miguel J and Gutierrez NC: Effects of IL-8 Up-regulation on cell survival and osteoclastogenesis in multiple myeloma. Am J Pathol 186: 2171-2182, 2016.
23. Gu JH, Tong XS, Chen GH, Liu XZ, Bian JC, Yuan Y and Liu ZP: Regulation of matrix metalloproteinase-9 protein expression by 1alpha,25-$(OH)_2D_3$ during osteoclast differentiation. J Vet Sci 15: 133-140, 2014.
24. Kim KW, Kim BM, Moon HW, Lee SH and Kim HR: Role of C-reactive protein in osteoclastogenesis in rheumatoid arthritis. Arthritis Res Ther 17: 41, 2015.
25. Gupta G: Gingival crevicular fluid as a periodontal diagnostic indicator-II: Inflammatory mediators, host-response modifiers and chair side diagnostic aids. J Med Life 6: 7-13, 2013.
26. Carneiro LG, Nouh H and Salih E: Quantitative gingival crevicular fluid proteome in health and periodontal disease using stable isotope chemistries and mass spectrometry. J Clin Periodontol 41: 733-747, 2014.
27. Silva-Boghossian CM, Colombo AP, Tanaka M, Rayo C, Xiao Y and Siqueira WL: Quantitative proteomic analysis of gingival crevicular fluid in different periodontal conditions. PLoS One 8: e75898, 2013.
28. Tsuchida S, Satoh M, Umemura H, Sogawa K, Kawashima Y, Kado S, Sawai S, Nishimura M, Kodera Y, Matsushita K and Nomura F: Proteomic analysis of gingival crevicular fluid for discovery of novel periodontal disease markers. Proteomics 12: 2190-2202, 2012.
29. Bostanci N, Heywood W, Mills K, Parkar M, Nibali L and Donos N: Application of label-free absolute quantitative proteomics in human gingival crevicular fluid by LC/MS E (gingival exudatome). J Proteome Res 9: 2191-2199, 2010.
30. Choi YJ, Heo SH, Lee JM and Cho JY: Identification of azurocidin as a potential periodontitis biomarker by a proteomic analysis of gingival crevicular fluid. Proteome Sci 9: 42, 2011.
31. Dings RPM, Miller MC, Griffin RJ and Mayo KH: Galectins as molecular targets for therapeutic intervention. Int J Mol Sci 19: 905, 2018.
32. Johannes L, Jacob R and Leffler H: Galectins at a glance. J Cell Sci 131: jcs208884, 2018.
33. Jacobs J and Braun J: The mucosal microbiome. In: Mucosal Immunology. Mestecky J, Strober W, Russell M, Cheroutre H, Lambrecht BN and Kelsall B (eds). 4th Edition. Academic Publishing, Cambridge, MA, USA.
34. Chou FC, Chen HY, Kuo CC and Sytwu HK: Role of galectins in tumors and in clinical immunotherapy. Int J Mol Sci 19: 430, 2018.
35. Dings RPM, Miller MC, Griffin RJ and Mayo KH: Galectins as molecular targets for therapeutic intervention. Int J Mol Sci 19: 905, 2018.
36. Helene F and Rosenberg: Suppression, surprise: Galectin-10 and treg cells. Blood 110: 1407-1408, 2007.
37. Muller J, Duray E, Lejeune M, Dubois S, Plougonven E, Léonard A, Storti P, Giuliani N, Cohen-Solal M, Hempel U, *et al*: Loss of stromal galectin-1 enhances multiple myeloma development: Emphasis on a role in osteoclasts. Cancers (Basel) 11: 261, 2019.
38. Vinik Y, Shatz-Azoulay H, Vivanti A, Hever N, Levy Y, Karmona R, Brumfeld V, Baraghithy S, Attar-Lamdar M, Boura-Halfon S, *et al*: The mammalian lectin galectin-8 induces RANKL expression, osteoclastogenesis, and bone mass reduction in mice. Elife 4: e05914, 2015.
39. Moriyama K, Kukita A, Li YJ, Uehara N, Zhang JQ, Takahashi I and Kukita T: Regulation of osteoclastogenesis through Tim-3: Possible involvement of the Tim-3/galectin-9 system in the modulation of inflammatory bone destruction. Lab Invest 94: 1200-1211, 2014.
40. Taba M Jr, Kinney J, Kim AS and Giannobile WV: Diagnostic biomarkers for oral and periodontal diseases. Dent Clin North Am 49: 551-571, vi, 2005.
41. Teles RP, Likhari V, Socransky SS and Haffajee AD: Salivary cytokine levels in subjects with chronic periodontitis and in periodontally healthy individuals: A cross-sectional study. J Periodontal Res 44: 411-417, 2009.